

Title: Prospective application, mechanism, and deficiency of lithium bis(oxalate)borate as the electrolyte additive for Lithium-batteries

Jianing Li^{a,#}, Jianzhong Yang^{b,#}, Zhaoqi Ji^{c,#}, Min Su^d, Huijing Li^a, Yanchao Wu^a, Xin Su^{e,}, Zhengcheng Zhang^{f,*}*

^a Advanced Battery Technology Center, School of Marine Science and Technology, Harbin Institute of Technology, Weihai 264209, P. R. China

^b R&D center, Shenzhen ORI Technology Company Limited, Shenzhen 518000, China

^c Advanced Fuel Cell Laboratory, School of Automotive Engineering, Harbin Institute of Technology (Weihai), Weihai 264209, China

^d R&D Center, Wanxiang A123 Systems Corp, Hangzhou, 311215, China

^e Advanced Battery Technology Center, School of New Energy, Harbin Institute of Technology, Weihai, 264209, China

^f Chemical Sciences and Engineering Division, Argonne National Laboratory, 9700 South Cass Avenue, Lemont, IL 60439-4837, USA

This is the author manuscript accepted for publication and has undergone full peer review but has not been through the copyediting, typesetting, pagination and proofreading process, which may lead to differences between this version and the [Version of Record](#). Please cite this article as [doi: 10.1002/aenm.202301422](https://doi.org/10.1002/aenm.202301422).

This article is protected by copyright. All rights reserved.

Keywords: lithium bis(oxalate)borate; solid electrolyte interphase; cathode electrolyte interphase; additive; lithium-ion battery

Author Manuscript

This article is protected by copyright. All rights reserved.

Abstract

Lithium bis(oxalate)borate (LiBOB) is one of the most common film-forming electrolyte additives used in lithium ion batteries (LIBs), since it can form a dense boron-containing polymer as a solid electrolyte interlayer (or cathode electrolyte interlayer) in order to isolate the electrode material from the electrolyte and prevent side reactions. LiBOB can serve as HF scavenger to maintain the structural integrity of electrodes via avoiding the transition metal dissolution caused by HF attack. LiBOB also can react with LiPF_6 to generate lithium difluoro (oxalate)borate (LiDFOB) that can be further used as a clean-up agent for reactive oxygen radicals. This article lists the application of LiBOB in high capacity and high voltage cathode materials, and also review the working mechanisms of LiBOB used in these materials to improve the performance of LIBs. At last, it presents the current shortcomings of LiBOB and strategies to overcome. This article will be expected to provide useful insights for employing LiBOB as a feasible method of dealing with the difficulty of running high capacity LIBs stably under high voltage.

This article is protected by copyright. All rights reserved.

Author Manuscript

1. Introduction

The capacity and voltage of cathode materials of lithium-ion batteries (LIBs) have been steadily increased with innovates in cathode materials.^[1, 2] High-capacity, nickel-rich, layered oxide cathode ($\text{LiNi}_x\text{Co}_y\text{Mn}_{1-x-y}\text{O}_2$, NCM) and lithium-rich layered oxides (LRLO) have attracted many attention and are widely used in lithium-ion batteries,^[3] however, the use of these materials face a substantial number of challenges.^[4, 5] Fore example, the nickel (Ni) in NCM materials is easy to dissolve into electrolyte and deposit on the graphite cathode, while cobalt content will be reduced, resulting in an unstable architecture of the NCM materials, which can easily react with electrolyte to reduce the capacity of LIBs.^[6, 7] Therefore, the electrolyte always needs additives to form a dense and homogeneous film that can isolate the electrolyte from the cathode material and prevent the influence of side reactions.^[8, 9] Lithium bis(oxalate)borate (LiBOB) is such a classic additive, used to improve the multiplicity and cycling performance of LIBs.^[10] It can form a passivated solid cathode electrolyte interface (CEI) containing elements of borate on cathode surface.^[11] This CEI film not only prevents the electrolyte from leaching to the boundaries, but it also eliminates undesirable reactions at the cathode-electrolyte interface.^[12] At the same time, it promotes the kinetics of Li^+ diffusion, ensuring better rate performance of NCM811.^[13]

Besides, although researchers have developed many lithium-rich layered oxides (LRLO) with higher specific capacities and higher electrochemical windows like $\text{Li}_{1.2}\text{Ni}_{0.13}\text{Mn}_{0.54}\text{Co}_{0.13}\text{O}_2$ ^[14], $\text{Li}_{1.141}\text{Mn}_{0.537}\text{Ni}_{0.265}\text{Co}_{0.057}\text{O}_2$ ^[15] and $\text{Li}_2\text{Ir}_{0.75}\text{Sn}_{0.25}\text{O}_3$, the severe dissolution of transition metals in lithium-rich layered oxides and the generation of oxygen vacancies and oxygen radicals lead to the rapid decay of capacity and voltage during cycling.^[10, 16] LiBOB can be applied in lithium-rich layered oxides to reduce the dissolution and redeposition of transition metals.^[17, 18] It has been proved that

This article is protected by copyright. All rights reserved.

it can serve as HF scavenger to reduce the HF corrosion on LRLO, so less transition metal dissolution and redeposition on the graphite was found.^[40] Besides, it was also found that it can be preferentially oxidized at LRLO surface to form a uniform protective film to maintain the structural integrity and suppress the transition metal dissolution.

Recently, a number of studies have found that LiBOB is used in high-voltage cathode materials, such as $\text{LiNi}_{0.5}\text{Mn}_{1.5}\text{O}_4$ (LNMO)^[19, 20], LiCoPO_4 ^[21], and LRLO^[18, 22], to improve cycling stability. So far, the beneficial effect of LiBOB on high-voltage batteries has mainly been in its ability to form CEI. Other recent studies have found that LiBOB can also act as a scavenger of HF and oxygen radicals.^[17, 23] However, the mechanism of its operation and the detailed strategies to its shortcomings have still not been reasonably explained. On this basis, this article summarizes the improvement of the electrochemical performance of LIBs with electrolyte containing LiBOB, describes the classical film formation mechanism of LiBOB, as well as the scavenging mechanism of HF and oxygen radicals via LiBOB. Finally, we also lists the shortcomings of LiBOB and comes up with some strategies as shown in Figure 1. The representative examples of lithium ion batteries employing electrolyte containing LiBOB are summarized in Figure 2.

2 Comparison of lithium salts: Lithium difluorosulfimide (LiFSI), LiPF_6 , LiBOB, LiBF_4 , LiDFOB

The lithium salt most commonly used at present is LiPF_6 ^[24-26], which has poor thermal and hydrolytic stability and decomposes to generate HF^[27]. The thermal stability of LiPF_6 solutions is poor, as LiPF_6 decomposes at 60 °C.^[24, 25] Because PF_6^- is a strong oxidative agent at high temperatures, LiPF_6 alkyl carbonate solutions undergo thermal runaway when heated, even when not in contact with the electrodes. Moreover, the decomposition of LiPF_6 generates HF, the presence

This article is protected by copyright. All rights reserved.

of which has an effect on both the cathode and the anode.^[28] It severely affects the passivation of graphite electrodes and accelerates the dissolution of transition metals from the cathode materials. Researchers have found that the presence of HF in LiPF₆ solutions is one of the main reasons for the poor performance of LIBs at high temperatures.^[27]

To solve the thermal runaway problem, researchers have discovered another lithium salt, LiFSI, which has a high decomposition temperature (>200°C) and better stability to moisture.^[29, 30] Also, the conductivity of LiFSI is 9.73 mS/cm, which is also higher than that of LiPF₆ at 9.33 mS/cm (1.0M lithium salt at EC/EMC = 3/7).^[31] However, the LiFSI synthesis process is still relatively expensive, and LiFSI tends to corrode the positive collector aluminum foil at high concentrations and voltages. Fortunately, researchers have found that adding a small amount of LiBOB as an additive or reducing the Cl⁻ impurities during the synthesis process can alleviate the corrosion.^{[30] [32-35]} Zhang et al. added 0.2 mol/L LiFSI to 1.0 mol/L LiPF₆-based electrolyte and found a significant improvement in cycle stability and multiplicative performance of the graphite negative electrode, while adding 0.2 mol/L LiBOB could passivate the surface of aluminum foil and mitigate the corrosion of LiFSI.^[32] LiBOB can react with the aluminium foil to form an AlBO₃ passivation layer, and on top of this a highly stable network structure is formed as a protective layer, which maximizes the isolation of the electrolyte and reduces the corrosion of the aluminium foil by the electrolyte.^[36]

Other lithium salts containing boron element such as LiBF₄ is also commonly used because of its good thermal and hydrolytic stability,^[37] and it also can passivate aluminum collectors and reduce corrosion of aluminum collectors.^[38] However, LiBF₄ has low electrical conductivity and is less compatible with graphite anodes in alkyl carbonates.^[37] Compared to LiBF₄, LiBOB not only has better thermal stability but also has a much better ability to passivate aluminum collectors than

This article is protected by copyright. All rights reserved.

LiBF₄.^[36, 39] In addition, LiBOB has more significant improvement in the electrochemical performance of both graphite and silicon anodes.

To solve the problem of HF generation and removal, Zhang et al.^[40] found that LiBOB can react with water to prevent the generation of HF, the exact mechanism of which is detailed in the section on the removal of HF (3.2 Removal mechanism of HF corrosion). In addition, LiBOB reacts with LiPF₆ to generate LiDFOB, which has the function of scavenging oxygen radicals, the mechanism of which is described in detail in the following section on scavenging oxygen radicals (3.3 Removal mechanisms of superoxide radicals in LiBOB and LiDFOB.) Zhang et al.^[40] found that LiBOB reacts with LiPF₆ to form LiDFOB *in situ*, which also forms CEI and SEI on cathode and anode surface, respectively, though the CEI formed by LiDFOB can be easily decomposed.^[40]

LiBOB has high thermal stability (302°C) and high conductivity at low cost. LiBOB is mainly suitable for solvents with high dielectric constants, while at the same time LiBOB can meet the requirements of high voltage cathode materials and can be used in electrolyte compositions^[41-43]. The high voltage cathodes materials usually suffer from structural damages caused by irreversible phase change and oxidative decomposition of electrolyte at high cut-off voltage. Therefore, it requires to inhibit the structural damage of cathode materials and mitigate the oxidative decomposition of electrolyte at high cut-off voltage. LiBOB can form a stable CEI to mitigate the oxidative decomposition of electrolyte, and this CEI can also allow large amounts of Li⁺ to be embedded and removed, which prevents the structural changes in cathode surface at high cut-off voltage. Meanwhile, the oxidative stability of LiBOB in lithium batteries is up to 5.3 V, significantly higher than the 4.5 V of LiPF₆.^[44, 45] These features explain why LiBOB is widely used in the field of battery.

This article is protected by copyright. All rights reserved.

In summary, LiBOB has better thermal stability with low cost than that of LiPF_6 , it also renders higher conductivity and better compatibility with graphite anodes than that of LiBF_4 . LiBOB itself can act as HF scavenger and form protective film to mitigate structural change of electrodes, which also can be used as additive or second salt to mix with advanced lithium salt LiFSI to prevent the aluminum corrosion at high cut-off voltage. At last, LiBOB can also react with LiPF_6 in situ to form LiDFOB to scavenge oxygen radicals.

3 Functional mechanisms of LiBOB

It is necessary to discuss the functional operations of LiBOB in details. The Dong lab's consistent testing and research on LiBOB, as well as research from Zhao et al. indicate that the LiBOB-containing electrolyte not only facilitates the formation of a denser solid electrolyte interface phase on anode surface but also forms a stable cathode electrolyte interface layer, effectively preventing corrosion at the cathode interface and significantly improving the long-term cycling performance of the battery. In-depth knowledge of these processes provides useful insights for continued study and future application.

3.1 Film formation mechanism

LiBOB is composed of Li, B and O (as shown in Figure 3a) with a HOMO of -6.45 eV (as shown in Figure 3b) that is higher than other electrolyte molecules^[46, 47]. LiBOB has a high HOMO and is electrochemically oxidized during charging before the electrolyte decomposes, forming an inorganic/polymer CEI rich in B and O on the electrode, which effectively eliminates unfavorable reactions at the cathode-electrolyte interface and prevents electrolyte penetration into the grain boundaries.^[48] LiBOB can form both CEI and SEI. The decomposition products of LiBOB can combine

This article is protected by copyright. All rights reserved.

to form dimers, but the BOB- in LiBOB reacts more readily with the solvent EC to form oligomers. LiBOB is then further oxidated and decomposed to long linear organic SEI films that attach to the active material by B-O bonds (as shown in Figure 3c.) resulting in a thick, soft SEI that contains more organic species, such as ROCO_2Li , and is more conducive to Li^+ transport to inhibit solvent diffusion to the electrode surface.^[36] Because of the strong B-O bond, this SEI film is difficult to detach from the material even after cycling through the charging and discharging processes. This effectively isolates the material from the electrolyte to prevent side reactions and keep long-time durability^[49].

LiBOB's excellent film-forming properties are suitable for employing with common high-voltage electrolytes and high-voltage materials. The application of LiBOB to high-voltage spinel $\text{LiNi}_{0.5}\text{Mn}_{1.5}\text{O}_4$ cathodes results in the formation of an organic-rich SEI layer that inhibits the dissolution of nickel and manganese with the oxidative decomposition of the electrolyte improving its electrochemical performance.^[50] LiBOB is applied to the high-capacity nickel-rich layered oxide cathode $\text{LiNi}_{0.8}\text{Co}_{0.1}\text{Mn}_{0.1}\text{O}_2$ (nickel-rich NCM), and the inorganic B and O-rich interfacial layer formed by LiBOB provides a fast Li^+ diffusion channel, ensuring high multiplicity performance of the nickel-rich NCM.^[48] The application of LiBOB to lithium-rich layered oxides results in the formation of B and O-rich inorganic boundary masks that enhance the stability of the interface, in addition to its ability to react with free radicals, greatly reducing gas generation and making the cycle more stable.^[40]

Fluorinated electrolytes based on fluorinated ethylene carbonate are considered a promising alternative to high-voltage and high-energy lithium batteries. However, because the introduction of fluorine decreases the lowest energy level of molecular orbitals in the solvent, the fluorinated ethylene carbonate is less resistant to reduction and so can lead to instability in graphite-negative electrodes.^[51] Propylene carbonate is poorly compatible with graphite and tends to reduce on

This article is protected by copyright. All rights reserved.

graphite and then become embedded with lithium ions between the graphite layers, a process that can lead to the destruction of the inner layer of the graphite negative electrode.^[52] ^[53] The electrolyte containing LiBOB can form a thick and soft SEI with more organic species, which can improve the performance of the graphite anode to remove PF₅ and prevent PC co-intercalation.^[50] LiBOB can be reduced at 1.6 V and forms a strong SEI on the graphite surface. This strong SEI successfully prevents the co-intercalation of propylene carbonate molecules with the graphite, greatly improving the durability of the SEI on the graphite negative electrode. In addition to its better compatibility with graphite anodes, LiBOB also renders improvement when employed in silicon anodes. Comparing with silicon anodes, LiBOB can form a layer of less porous SEI, reducing the electrochemically inactive silicon phase,^[54] so the SEI formed by LiBOB becomes highly conductive. Besides, it also can inhibit the oxidation of the electrolyte and reduce the dissolution of Ni,Co,Mn on the cathode.

3.2 Removal mechanism of HF corrosion

Another important way in reducing the dissolution of transition metals, in addition to form a stable CEI and reduce the structural damage on cathode, is to remove corrosion caused by HF. HF continues to corrode the interfacial film during the cell cycle as the cathode oxide is corroded, transition metal ions dissolve into the electrolyte and deposit onto the graphite, eventually leading to graphite poisoning.^[44] The transformation of the transition metal elements can be catalyzed by the amount of HF generated, which will ultimately lead to the destruction of the protective film and further decomposition of the electrolyte.^[55, 56]

This article is protected by copyright. All rights reserved.

The study has demonstrated that electrons are released not only from the cathode but also possibly from the ethylene carbonate (EC) during high-voltage charging, which leads to the oxidation and structural destruction of EC molecules to open the ring and react with water, producing protons as shown in Figure 4d.^[26, 57] The protons come to the surface of cathodes and combine with the oxygen to produce more water. The H₂O will then hydrolyze the LiPF₆ salt or PF₅ in the electrolyte and form HF, which in turn, corrodes the CEI and oxide cathodes, generating more H₂O (as shown in Figure 4e.)^[26, 58] So the loose CEI formed on the surface of the cathode is corroded by HF, resulting in severe deformation.

To reduce the corrosion of HF while forming an interfacial film, LiBOB is used as an additive. LiBOB decomposes during charging and the borate or boric acid produced by the decomposition of LiBOB can react with the HF produced by LiPF₆ to form LiBF₄ and LiDFOB.^[59] Thermodynamically, the production energy of BF₄⁻ is much lower than that of HF, so BF₄⁻ is more readily available, and the bond energy of B-F is much higher than that of H-F and P-F, implying that a more stable product is generated that is more difficult to decompose^[60, 61]. The reduced amount of HF corrosion in the LiBOB electrolyte allows for the formation of a more uniform SEI on the graphite surface. In a full cell using LiBOB electrolyte, the dissolution of transition metal ions in the electrolyte and their deposition on the graphite are reduced due to less HF attack on the CEI and SEI, improving the cycling stability of the high voltage cathode.^[62, 63]

3.3 Removal mechanisms of superoxide radicals in LiBOB and LiDFOB

LiDFOB, generated by LiBOB and LiPF₆ in the electrolyte, can clean up oxygen radicals, thus preventing the production of gases such as oxygen and carbon dioxide.^[40, 62] Alternatively, LiDFOB

This article is protected by copyright. All rights reserved.

can directly add into the electrolyte to effectively remove the nucleophilic species and their parasitic reactions (as shown in Figure 5a.) However, the decomposition products of LiDFOB are soluble boron-containing oligomers that are useless for further formation of CEI. The thinner CEI is ineffective in protecting the electrode materials during cycling, resulting in the decomposition and deformation of cathodes^[18]. As for LiBOB, it can deeply remove oxygen radicals just like LiDFOB. On the other hand, the unique advantage of LiBOB, is that the decomposition products are insoluble boron-containing polymers, which in turn can form a homogeneous and thick CEI in Figure 5b and Figure 4 j and k.^[63] These CEI films avoid direct contact between the electrolyte and the LRLO as much as possible, preventing the side reactions. At the same time, the films are an organic polymer containing B or F, which facilitates the efficient transfer of lithium ions and improves the electrochemical stability of the cathode materials (as shown in Figure 4 f–i.) The electrolyte containing LiBOB also has a lower impedance, as can be seen from the electrochemical impedance diagram shown in Figure 5h. The thickness of electrolyte films also affects the performance of LIBs in Figure 5 c–e and Figure 4 a–c. The film formed by LiBOB is the thickest (Figure 5 c–e) and therefore is more likely to keep stable and not deteriorate during long-time cycling (Figure 5 f and g)^[64].

4 Challenges and Strategies for LiBOB

LiBOB has many advantages over its current alternatives, such as more effective inhibition of Mn^{3+} dissolution compared to $LiPF_6$, better thermal stability, higher compatibility with cathode and anode materials, non-corrosive to manganese and iron cathode materials, as well as being fluorine-free and non-toxic. However, LiBOB also has disadvantages: its poor solubility in certain low dielectric constant solvents and its lower ionic conductivity (compared to $LiPF_6$ -based electrolytes)

This article is protected by copyright. All rights reserved.

are key factors that hindering its large-scale production. Low ionic conductivity and poor diffusion of lithium ions increase the internal resistance of the battery and increase the polarization of the battery, which in turn affects the multiplicity and low temperature performance of the battery.^[65] In addition to aforementioned drawbacks, the low Coulomb efficiency of LiBOB at voltages above 4.7V, and impurities such as water that are difficult to remove during synthesis, which also affect its performance.

It has been shown that LiBOB improves initial Coulomb efficiency and cycling performance at lower potential (<4.7V) (shown in Figure 5a–c) through forming an effective SEI isolation electrolyte and inhibiting side reactions (as in Figure 6 i–l).^[66, 67] However, LiBOB-SEI is unstable and decomposes at higher potentials (>4.7V), as shown in Figure 6g and h. Only a small amount is still remaining and not enough to adequately protect the electrodes (shown in Figure 6m–q.)^[10, 68] The electrolyte will then directly contact with the electrode, creating side reactions and causing a rapid decrease of electrochemical performance (as shown in Figure 6d–f.)^[10] A way to address this challenge is to use a combination of additives. It has been proven that LiDFP can be used in conjunction with LiBOB to form a more stable SEI for high voltage application, increasing the cycle stability and providing better cycling durability at 4.8V.^{[69], [70]} The other challenge is that impurities in LiBOB will increase the impedance of LIBs, which lead to a decline in electrochemical performance. Thus, it is also important to improve the purity of LiBOB. In the traditional method of LiBOB synthesis, LiBOB·H₂O is present as a by-product, which reduces the purity of LiBOB and affects the performance of lithium batteries.^[17] Therefore, it is essential to remove the water molecules from the LiBOB during synthesis. Yarpark et al.^[71] obtained high purity LiBOB (>99%) by recrystallization under protective atmosphere of argon and avoiding the adverse effects of

This article is protected by copyright. All rights reserved.

impurities such as corrosion of electrodes, dissolution of transition metals, generation of free radicals and HF in electrolyte. Lithium carbonate, oxalic acid and boric acid is used as raw materials for the synthesis of LiBOB under a protective atmosphere, by using ceramic processing method and consequently avoiding the by-product $\text{LiBOB}\cdot\text{H}_2\text{O}$.^[72] The development of anhydrous synthesis processes is the trend in this field.

LiBOB, a classic additive, has been used from the initial LiCoO_2 and NCM, to nickel-rich layered oxide cathode and lithium-rich layered oxides batteries with higher theoretical capacities, because it can prevent side reactions by forming protective SEI/CEI to isolate the contact of electrolytes and electrodes. LiBOB can also remove corrosive substances such as HF. The LiDFOB generated by LiBOB reacting with LiPF_6 can remove superoxide radicals as well, which greatly reduce the production of extraneous gases such as carbon dioxide in LIBs. Compared with adding LiDFOB directly into LIBs, CEI formed by LiBOB is thicker and more homogeneous, providing better protection for the electrodes and improving the durability of LIBs during cycling. LiBOB therefore has promising applications and market prospects. First, the application of LiBOB provides a simple solution to address the severe electrolyte decomposition in high-energy lithium batteries. The potential mechanisms found by LiBOB provide useful insights for rational design of the lithium-anode interface. Secondly, LiBOB acts as a scavenger of HF in high-voltage cells thereby improving the cycling stability of laminated oxide cells. This finding shows that LiBOB can be applied to high voltage systems such as layered oxides, like spinel LNMO or LiCoMnO_4 , olivine LiCoO_4 , etc., thus possibly opening the door to the commercialization of these high voltage cathode materials. This work also provides useful guides for future exploration of new materials to stabilize LiPF_6 's carbon-based electrolyte by removing or deactivating the reactive materials generated during electrolyte decomposition.

This article is protected by copyright. All rights reserved.

Acknowledgments

Jianing Li, Jianzhong Yang, and Zhaoqi Ji contributed equally. X. S. would like to thank the support of the Young Taishan Scholars Program of Shandong Province and the Shandong Provincial Natural Science Foundation (2022HWYQ-074). Z. Z. gratefully acknowledges the support from the U.S. Department of Energy's (DOE) office of Energy Efficiency & Renewable Energy (EERE) Vehicle Technologies Office. Argonne National Laboratory is a U.S. Department of Energy Office of Science Laboratory operated under Contract No. DE-AC02-06CH11357.

Received: ((will be filled in by the editorial staff))

Revised: ((will be filled in by the editorial staff))

Published online: ((will be filled in by the editorial staff))

This article is protected by copyright. All rights reserved.

Author Manuscript

References

- [1]. K. Guo, C. Zhu, H. Wang, S. Qi, J. Huang, D. Wu, J. Ma, *Adv. Energy Mater.* **2023**, 2204272.
- [2]. R. Sim, L. Su, A. Manthiram, *Adv. Energy Mater.* **2023**, 2300096.
- [3]. W. Li, X. Liu, H. Celio, P. Smith, A. Dolocan, M. Chi, A. Manthiram, *Adv. Energy Mater.* **2018**, 8, 1703154.
- [4]. S. Klein, P. Harte, J. Henschel, P. Bärmann, K. Borzutzki, T. Beuse, S. Wickeren, B. Heidrich, J. Kasnatscheew, S. Nowak, M. Winter, T. Placke, *Adv. Energy Mater.* **2021**, 11, 2003756.
- [5]. Z. Chen, G.-T. Kim, D. Bresser, T. Diemant, J. Asenbauer, S. Jeong, M. Copley, R. J. Behm, J. Lin, Z. Shen, S. Passerini, *Adv. Energy Mater.* **2018**, 8, 1801573.
- [6]. Z. Xu, X. Guo, J. Wang, Y. Yuan, Q. Sun, R. Tian, H. Yang, J. Lu, *Adv. Energy Mater.* **2022**, 12, 2201323.
- [7]. Y. Shi, M. Zhang, Y. S. Meng, Z. Chen, *Adv. Energy Mater.* **2019**, 9, 1900454.
- [8]. S. Lin, H. Hua, P. Lai, J. Zhao, *Adv. Energy Mater.* **2021**, 11, 2101775.
- [9]. J. G. Han, C. Hwang, S. H. Kim, C. Park, J. Kim, G. Y. Jung, K. Baek, S. Chae, S. J. Kang, J. Cho, S. K. Kwak, H. K. Song, N. S. Choi, *Adv. Energy Mater.* **2020**, 10, 2000563.

This article is protected by copyright. All rights reserved.

- [10]. J. Li, W. Li, Y. You, A. Manthiram, *Adv. Energy Mater.* **2018**, *8*, 1801957.
- [11]. X. Li, J. Zheng, X. Ren, M. H. Engelhard, W. Zhao, Q. Li, J. G. Zhang, W. Xu, *Adv. Energy Mater.* **2018**, *8*, 1703022.
- [12]. W. Zhao, J. Zheng, L. Zou, H. Jia, B. Liu, H. Wang, M. H. Engelhard, C. Wang, W. Xu, Y. Yang, J. G. Zhang, *Adv. Energy Mater.* **2018**, *8*, 1800297.
- [13]. Y. Li, W. Li, R. Shimizu, D. Cheng, H. Nguyen, J. Paulsen, S. Kumakura, M. Zhang, Y. S. Meng, *Adv. Energy Mater.* **2022**, *12*, 2103033.
- [14]. T. Liu, J. Liu, L. Li, L. Yu, J. Diao, T. Zhou, S. Li, A. Dai, W. Zhao, S. Xu, Y. Ren, L. Wang, T. Wu, R. Qi, Y. Xiao, J. Zheng, W. Cha, R. Harder, I. Robinson, J. Wen, J. Lu, F. Pan, K. Amine, *Nature* **2022**, *606*, 305.
- [15]. G. Li, Z. Ren, A. Li, R. Yu, W. Quan, C. Wang, T. Lin, D. Yi, Y. Liu, Q. Zhang, J. Wang, H. Yu, X. Sun, *Nano Energy* **2022**, *98*, 107169.
- [16]. M. Matsui, K. Dokko, Y. Akita, H. Munakata, K. Kanamura, *J. Power Sources* **2012**, *210*, 60.
- [17]. F. Lian, Y. Li, Y. He, H. Guan, K. Yan, W. Qiu, K. Chou, P. Axmann, M. Wohlfahrt-Mehrens, *RSC Adv.* **2015**, *5*, 86763.
- [18]. Z. Xiao, J. Liu, G. Fan, M. Yu, J. Liu, X. Gou, M. Yuan, F. Cheng, *Mater. Chem. Front.* **2020**, *4*, 1689.
- [19]. M. Xu, L. Zhou, Y. Dong, Y. Chen, A. Garsuch, B. L. Lucht, *J. Electrochem Soc.* **2013**,

160, A2005.

- [20]. S. Dalavi, M. Xu, B. Knight, B. L. Lucht, *Electrochem. Solid-State Lett.* **2011**, *15*, A28.
- [21]. V. Aravindan, Y. L. Cheah, W. C. Ling, S. Madhavi, *J. Electrochem. Soc.* **2012**, *159*, A1435.
- [22]. X. Bian, S. Ge, Q. Pang, K. Zhu, Y. Wei, B. Zou, F. Du, D. Zhang, G. Chen, *J. Alloys Compd.* **2018**, *736*, 136.
- [23]. J. Cha, J. G. Han, J. Hwang, J. Cho, N. S. Choi, *J. Power Sources* **2017**, *357*, 97.
- [24]. Z. Chen, N. Xu, W. Li, R. Zhao, Y. Dong, J. Liu, C. Su, J. Wang, C. Zhang, *J. Mater. Chem. A* **2019**, *7*, 16347.
- [25]. H. Jia, B. Billmann, H. Onishi, J. Smiatek, S. Roeser, S. Wiemers-Meyer, R. Wagner, M. Winter, I. Cekic-Laskovic, *Chem. Mater.* **2019**, *31*, 4025.
- [26]. M. Liu, J. Vatamanu, X. Chen, L. Xing, K. Xu, W. Li, *ACS Energy Lett.* **2021**, *6*, 2096.
- [27]. D. T. Shieh, P. H. Hsieh, M. H. Yang, *J. Power Sources* **2007**, *174*, 663.
- [28]. B. Philippe, R. m. Dedryvère, M. Gorgoi, H. k. Rensmo, D. Gonbeau, K. Edström, *J. Am. Chem. Soc.* **2013**, *135*, 9829.
- [29]. Y. Gao, Z. Zhai, K. Huang, Y. Zhang, *New J. Chem.* **2017**, *41*, 11456.
- [30]. S. J. Kang, K. Park, S. H. Park, H. Lee, *Electrochim. Acta* **2018**, *259*, 949.

This article is protected by copyright. All rights reserved.

- [31]. H. Han, S. Zhou, D. Zhang, S. Feng, L. Li, K. Liu, W. Feng, J. Nie, H. Li, X. Huang, *J. Power Sources* **2011**, *196*, 3623.
- [32]. L. Zhang, L. Chai, L. Zhang, M. Shen, X. Zhang, V. S. Battaglia, T. Stephenson, H. Zheng, *Electrochim. Acta* **2014**, *127*, 39.
- [33]. X. Shangguan, G. Jia, F. Li, Q. Wang, B. Bai, *J. Electrochem. Soc.* **2016**, *163*, A2797.
- [34]. K. Park, S. Yu, C. Lee, H. Lee, *J. Power Sources* **2015**, *296*, 197.
- [35]. R. Wang, X. Li, Z. Wang, H. Guo, M. Su, T. Hou, *J. Alloys Compd.* **2015**, *624*, 74.
- [36]. A. Hofmann, M. Schulz, V. Winkler, T. Hanemann, *J. Electrochem. Soc.* **2014**, *161*, A431-A438.
- [37]. L. D. Ellis, I. G. Hill, K. L. Gering, J. R. Dahn, *J. Electrochem. Soc.* **2017**, *164*, A2426-A2433.
- [38]. Z. Zhang, X. Chen, F. Li, Y. Lai, J. Li, P. Liu, X. Wang, *J. Power Sources* **2010**, *195*, 7397-7402.
- [39]. G. Xu, X. Shangguan, S. Dong, X. Zhou, G. Cui, *Angew Chem Int Ed Engl* **2020**, *59*, 3400-3415.
- [40]. B. Zhang, L. Wang, X. Wang, S. Zhou, A. Fu, Y. Yan, Q. Wang, Q. Xie, D. Peng, Y. Qiao, *Energy Storage Mater.* **2022**, *53*, 492.
- [41]. a. J. Jiang, J. Dahn, *Electrochem. Solid-State Lett.* **2003**, *6*, A180.

- [42]. L. Yang, P. Wang, D. Zhao, Y. Wei, Y. Han, S. Zeng, C. Wang, S. Li, *Sustainable Energy Fuels* **2020**, *4*, 4126.
- [43]. A. C. Kucuk, T. Minato, T. Yamanaka, T. Abe, *J. Mater. Chem. A* **2019**, *7*, 8559.
- [44]. X. Fan, C. Wang, *Che. Soc. Rev.* **2021**, *50*, 10486-10566.
- [45]. X. Cui, H. Zhang, S. Li, X. Li, H. Feng, *Ionics* **2014**, *20*, 789.
- [46]. H. Q. Pham, K. M. Nam, E. H. Hwang, Y. G. Kwon, H. M. Jung, S. W. Song, *J. Electrochem. Soc.* **2014**, *161*, A2002.
- [47]. D. Song, Z. Yang, Q. Zhao, X. Sun, Y. Wu, Y. Zhang, J. Gao, C. Wang, L. Yang, T. Ohsaka, F. Matsumoto, J. Wu, *ACS Appl. Mater. Interfaces* **2022**, *14*, 12264.
- [48]. F. Cheng, X. Zhang, Y. Qiu, J. Zhang, Y. Liu, P. Wei, M. Ou, S. Sun, Y. Xu, Q. Li, C. Fang, J. Han, Y. Huang, *Nano Energy* **2021**, *88*, 106301.
- [49]. Z. Du, D. L. Wood, I. Belharouak, *Electrochem. Commun.* **2019**, *103*, 109.
- [50]. S.-Y. Ha, J.-G. Han, Y.-M. Song, M.-J. Chun, S.-I. Han, W.-C. Shin, N.-S. Choi, *Electrochimica Acta* **2013**, *104*, 170-177.
- [51]. L. Xia, S. Lee, Y. Jiang, Y. Xia, G. Z. Chen, Z. Liu, *ACS omega* **2017**, *2*, 8741.
- [52]. G. Yan, X. Li, Z. Wang, H. Guo, J. Wang, *J. Phys. Chem. C* **2014**, *118*, 6586.
- [53]. R. Wagner, S. Brox, J. Kasnatscheew, D. R. Gallus, M. Amereller, I. Cekic-Laskovic, M. Winter, *Electrochem. Commun.* **2014**, *40*, 80.

- [54]. N.-S. Choi, K. H. Yew, H. Kim, S.-S. Kim, W.-U. Choi, *J. Power Sources* **2007**, *172*, 404-409.
- [55]. S. Li, J. Liu, L. Li, X. Li, J. Jing, X. Cui, *Appl. Surf. Sci.* **2015**, *330*, 316.
- [56]. D. J. Lee, J. Hassoun, S. Panero, Y. K. Sun, B. Scrosati, *Electrochem. Commun.* **2012**, *14*, 43.
- [57]. C. Zhan, T. Wu, J. Lu, K. Amine, *Energy Environ. Sci.* **2018**, *11*, 243.
- [58]. J. Zhang, J. Yang, L. Yang, H. Lu, H. Liu, B. Zheng, *Mater. Adv.* **2021**, *2*, 1747.
- [59]. J. Asenbauer, T. Eisenmann, M. Kuenzel, A. Kazzazi, Z. Chen, D. Bresser, *Sustainable Energy Fuels* **2020**, *4*, 5387.
- [60]. J. Lan, Q. Zheng, H. Zhou, J. Li, L. Xing, K. Xu, W. Fan, L. Yu, W. Li, *ACS Appl. Mater. Interfaces* **2019**, *11*, 28841.
- [61]. M. Metzger, B. Strehle, S. Solchenbach, H. A. Gasteiger, *J. Electrochem. Soc.* **2016**, *163*, A1219.
- [62]. S. Huang, S. Wang, G. Hu, L.-Z. Cheong, C. Shen, *Appl. Surf. Sci.* **2018**, *441*, 265.
- [63]. Y. Li, W. Li, R. Shimizu, D. Cheng, H. Nguyen, J. Paulsen, S. Kumakura, M. Zhang, Y. S. Meng, *Adv. Energy Mater.* **2022**, *12*, 2103033.
- [64]. X. Yu, A. Manthiram, *Energy Environ. Sci.* **2018**, *11*, 527.
- [65]. Q. Zhao, X. Li, F. Tang, D. Zhao, S. Du, S. Geng, Y. Tian, S. Li, *Energy Technol.* **2017**,

5, 406.

- [66]. M. Hong, S. Lee, V.-C. Ho, D. Lee, S.-H. Yu, J. Mun, *ACS Appl. Mater. Interfaces* **2022**, *14*, 10267.
- [67]. H. Zhao, X. Yu, J. Li, B. Li, H. Shao, L. Li, Y. Deng, *J. Mater. Chem. A* **2019**, *7*, 8700.
- [68]. Y. Dong, B. T. Young, Y. Zhang, T. Yoon, D. R. Heskett, Y. Hu, B. L. Lucht, *ACS Appl. Mater. Interfaces* **2017**, *9*, 20467.
- [69]. E. Hu, K. Xu, *Nat. Energy* **2022**, *7*, 482.
- [70]. D. Y. Wang, N. Sinha, R. Petibon, J. Burns, J. Dahn, *J. Power Sources* **2014**, *251*, 311.
- [71]. Y. Subaşı, S. Afyon, *ACS Appl. Energy Mater.* **2022**, *5*, 10098.
- [72]. C. Zor, Y. Subaşı, D. Hacıu, M. Somer, S. Afyon, *J. Phys. Chem. C* **2021**, *125*, 11310.

Author Manuscript

This article is protected by copyright. All rights reserved.

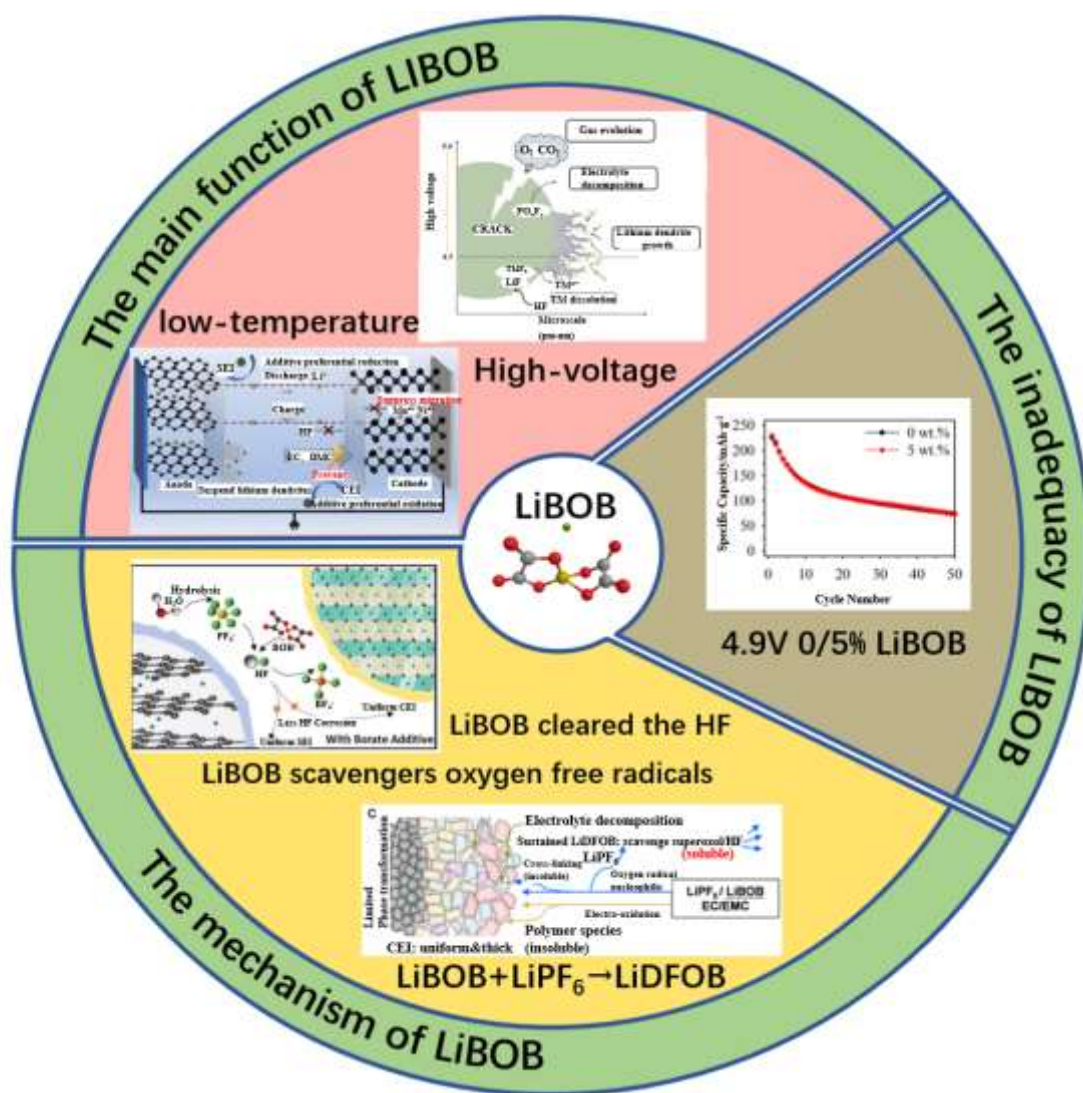


Figure 1 Application, mechanism and deficiency of LiBOB^[40, 63, 74]. Copyright 2022 Wiley Publishing.

Copyright 2022 ACS Publishing. Copyright 2022 ELSEVIER Publishing.

Author

This article is protected by copyright. All rights reserved.

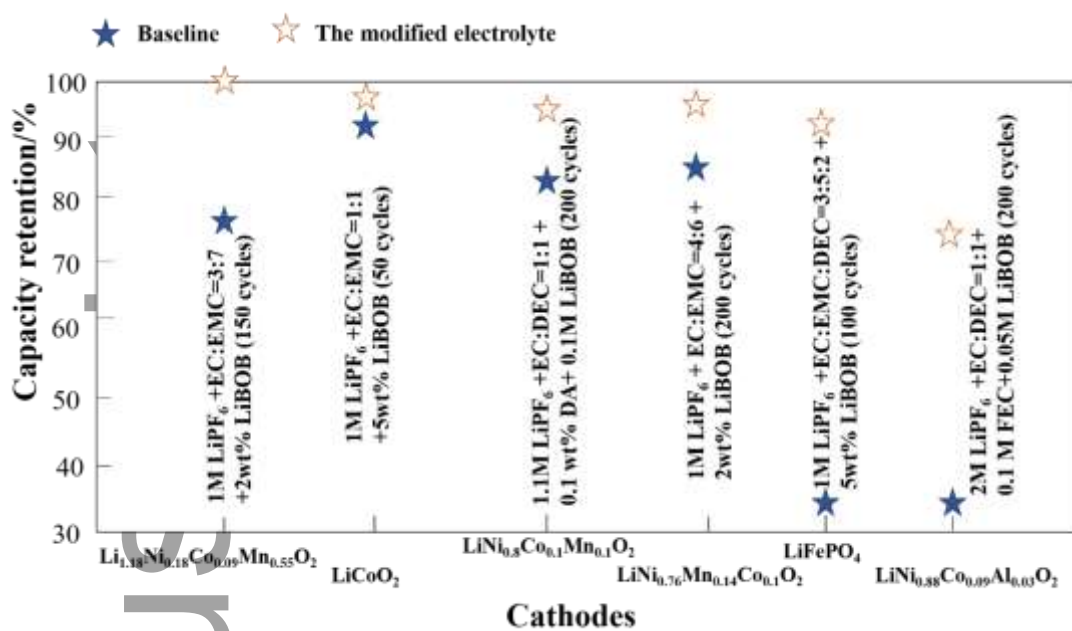


Figure 2 The performance of LiBOB in different cathodes and electrolytes. [48, 63, 74-77]

Author Manuscript

This article is protected by copyright. All rights reserved.

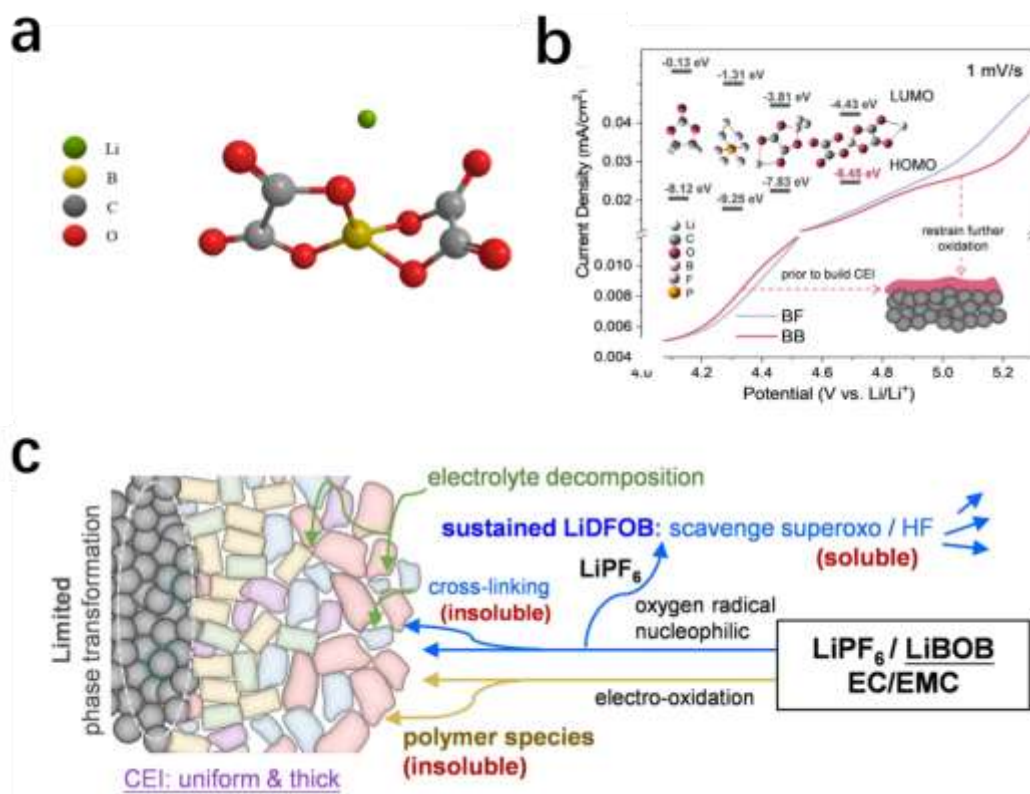


Figure 3 a Structural formulae of LiBOB.^[74] b shows the LSV of the stainless steel sheet electrode was measured at a constant scan rate of 1 mV/s. HOMO and LUMO energies were calculated for EC, LiPF₆, LiDFOB and LiBOB.^[40] c shows the scheme of cathode electrolyte interphase (CEI) formation and evolution on LRLO cathodes as concluded from characterization data in various electrolytes^[40] and LiBOB-contained electrolytes. Copyright 2022 ACS Publishing. Copyright 2022 ELSEVIER Publishing.

This article is protected by copyright. All rights reserved.

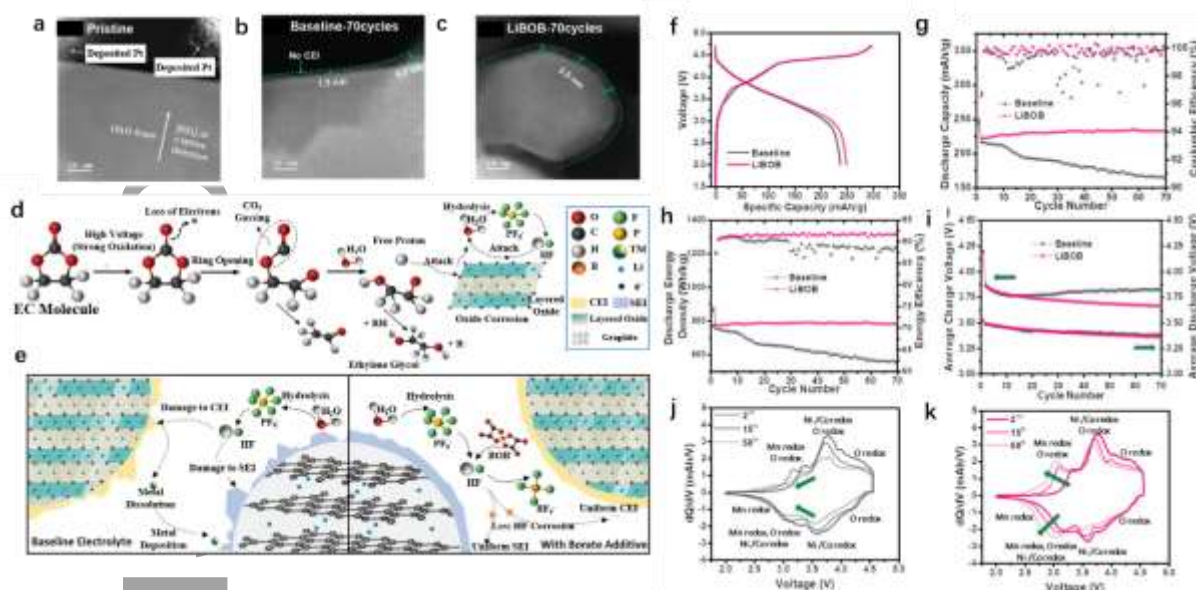


Figure 4 Cryogenic scanning electron microscopy images of the surface and/or CEI regions of LRLO cathode samples in different states^[63]: **a** pristine state, **b** cycling in baseline electrolyte, **c** cycling in LIBOB electrolyte. **d** Schematic mechanism of decomposition of carbonate-based electrolytes in high voltage layered oxide systems. **e** Mechanism of enhanced cell performance of borate-additive electrolytes in high voltage full cell systems. Electrochemical performance of LRLO-UM/graphite full cells in baseline electrolyte and LiBOB electrolyte: **f** first cycle voltage distribution, **g** cycle discharge capacity and CE, **h** cycle discharge energy density and EE, **i** cycle average charge/discharge voltage, **j** DQ/dV analysis of cell cycles in baseline electrolyte, **k** DQ/dV analysis of cell cycles in LiBOB electrolyte. All cells were 3 mAh cm⁻² level LRLO-UM/graphite full cells with 2-4.7 V, C/20 for the first cycle and 2-4.55 V, C/10 for the remaining cycles (1C = 270 mA g⁻¹). Copyright 2022 Wiley Publishing.

This article is protected by copyright. All rights reserved.

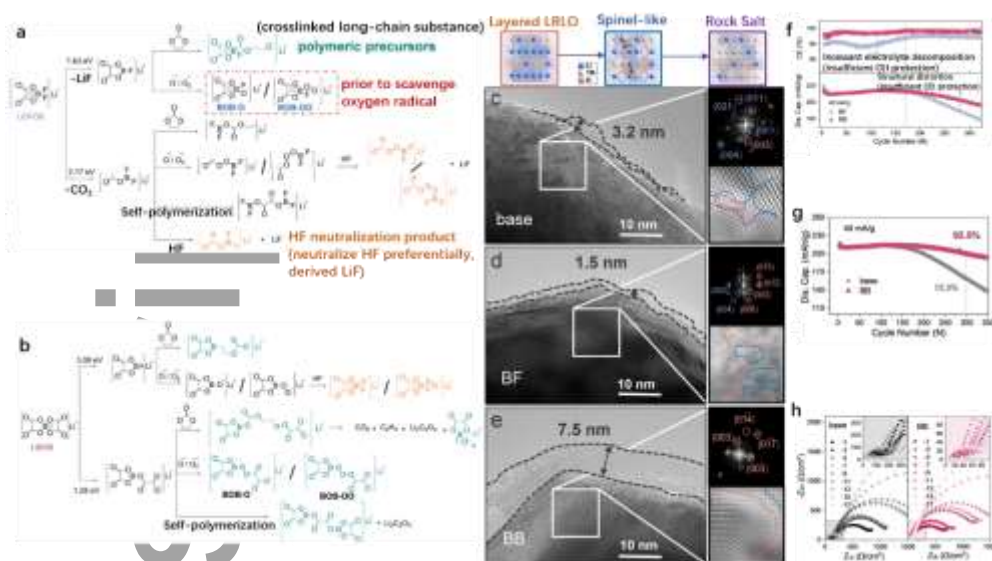


Figure 5 **a b** Possible reaction schemes for LiBOB and LiDFOB on LRLO. The cross-linking product is labelled in green, the HF neutralisation product in orange, and the ROS scavenging product in red. **c–e** TEM images of LRLO after 200 cycles with BB, BF and base electrolyte, crystal structure map and FFT. IFFT is also listed in the figure. The red grounded areas are identified as lamellar structures, blue is defined as spinel-like phases, and purple is assessed as rock salt structures. **f** Cycling performance of LRLO in BB (red) and BF (purple) under constant current discharge conditions at 40 mA/g. **g** Cycling capacity of LRLO/Li cells in base and BB at 40 mA/g discharge current. **h** Nyquist plots of LRLO in base and BB at different OCVs obtained from GITT-EIS at first charge. The region of higher frequencies is magnified. ^[40] Copyright 2022 ELSEVIER Publishing.

This article is protected by copyright. All rights reserved.

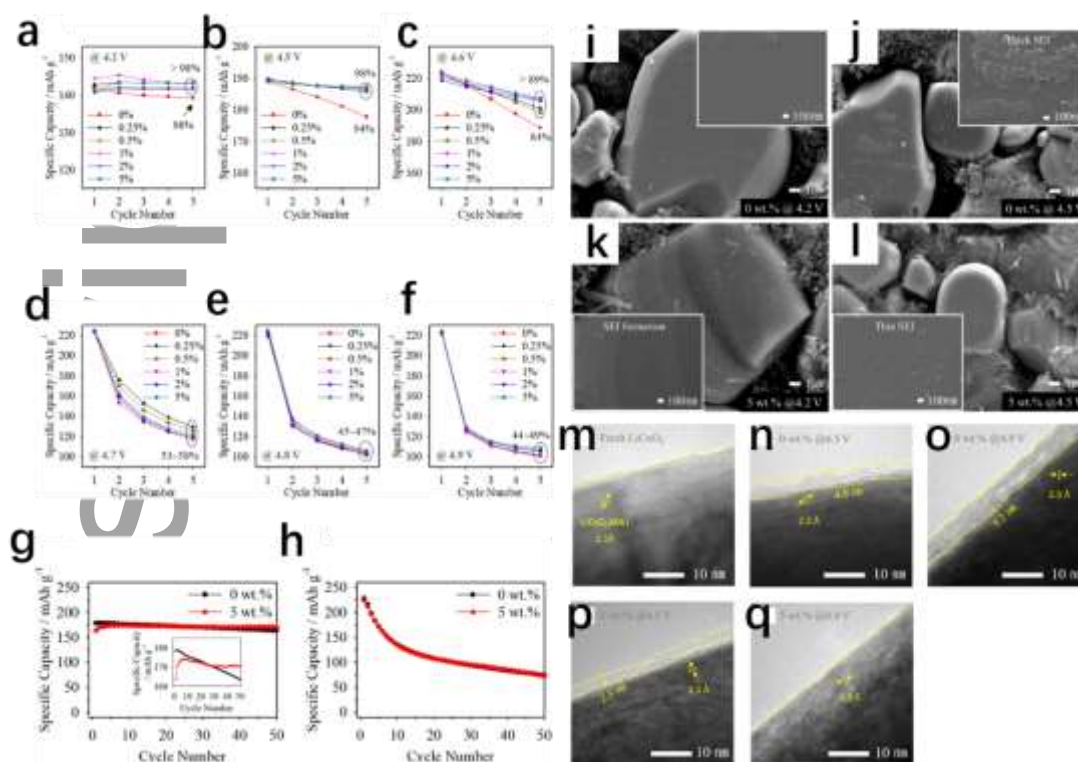


Figure 6 Discharge capacity of LCO at different voltage conditions of **a** 4.2V, **b** 4.5V, **c** 4.6V, **d** 4.7V, **e** 4.8V and **f** 4.9V for different concentrations of LiBOB in five cycles. **i** 0wt% and **j** 5wt% LiBOB cycled at 4.2V and 4.5V, respectively, and **k** 0wt% and **l** 5wt% LiBOB cycled at 4.5V, respectively. HR-TEM images of LCO particles were obtained under different conditions: **m** fresh LCO powder, **n** circulating electrode particles containing 0 wt% LiBOB at 4.5V and **o** 4.9V cutting voltage, **p** circulating electrode particles containing 5 wt% LiBOB at 4.5V and **q** 4.9V. ^[74] Copyright 2022 ACS Publishing.



This article is protected by copyright. All rights reserved.

Prof. Xin Su is the director of the Advanced Battery Technology Center, Harbin Institute of Technology, Weihai, with 15+ years of academic and industrial research and development (R&D) experience (from Brown University, Argonne National Lab, A123 systems LLC to Harbin Institute of Technology) in the field of battery materials and the design of lithium batteries. His current focus is materials and design of lithium batteries for various applications, including fundamental research, applied R&D, and manufacturing.

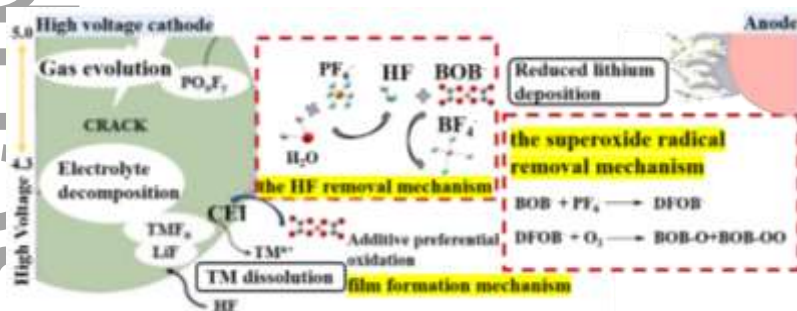


Dr. Zhengcheng (John) Zhang is a Senior Chemist/Group leader of Advanced Electrolyte Research Group at Argonne National Laboratory. He received his Ph.D. degree in polymer chemistry from Institute of Chemistry, Chinese Academy of Sciences in 2000. He has 25 years of experience in organic energy materials research for electrochemical energy storage. His research focuses on the design, synthesis and characterization of new organic materials for high-voltage high-energy Li-ion batteries and beyond such as Li-S batteries, sodium-ion battery, multivalent-ion battery, and redox flow batteries.

This review summarizes the current application of LiBOB in various high voltage cathodes, and compares the advantages and disadvantages of commonly used lithium salts with LiBOB. The

This article is protected by copyright. All rights reserved.

functional mechanism of LiBOB is then discussed in three aspects: the classical film formation mechanism; the HF removal mechanism; and the superoxide radical removal mechanism. Finally, the current challenges and strategies for LiBOB are presented.



This article is protected by copyright. All rights reserved.

Author Manuscript